Earth Planets Space, **58**, 1123–1130, 2006

Observations of the lower thermospheric neutral temperature and density in the DELTA campaign

Junichi Kurihara[1], Takumi Abe[1], Koh-Ichiro Oyama[1], Eoghan Griffin[2], Mike Kosch[3], Anasuya Aruliah[2], Kirsti Kauristie[4], Yasunobu Ogawa[5], Sayaka Komada[6], and Naomoto Iwagami[6]

[1]*Institute of Space and Astronautical Science, Japan Aerospace Exploration Agency, Sagamihara, Kanagawa 229-8510, Japan*
[2]*Atmospheric Physics Laboratory, University College London, 67-73 Riding House Street, London W1W 7EJ, U.K.*
[3]*Communication Systems, Lancaster University, Lancaster LA1 4WA, U.K.*
[4]*Finnish Meteorological Institute, P. O. Box 503, FIN-00101, Helsinki, Finland*
[5]*Solar-Terrestrial Environment Laboratory, Nagoya University, Chikusa-ku, Nagoya 464-8601, Japan*
[6]*Department of Earth and Planetary Science, Graduate School of Science, University of Tokyo, Bunkyo-ku, Tokyo 113-0033, Japan*

(Received October 2, 2005; Revised May 28, 2006; Accepted June 3, 2006; Online published September 29, 2006)

The rotational temperature and number density of molecular nitrogen (N_2) in the lower thermosphere were measured by the N_2 temperature instrument onboard the S-310-35 sounding rocket, which was launched from Andøya at 0:33 UT on 13 December 2004, during the Dynamics and Energetics of the Lower Thermosphere in Aurora (DELTA) campaign. The rotational temperature measured at altitudes between 95 and 140 km, which is expected to be equal to neutral temperature, is much higher than neutral temperature from the Mass Spectrometer Incoherent Scatter (MSIS) model. Neutral temperatures in the lower thermosphere were observed using the auroral green line at 557.7 nm by two Fabry-Perot Interferometers (FPIs) at Skibotn and the Kiruna Esrange Optical Platform System site. The neutral temperatures derived from the look directions closest to the rocket correspond to the rotational temperature measured at an altitude of 120 km. In addition, a combination of the all-sky camera images at 557.7 nm observed at two stations, Kilpisjärvi and Muonio, suggests that the effective altitude of the auroral arcs at the time of the launch is about 120 km. The FPI temperature observations are consistent with the in situ rocket observations rather than the MSIS model.

Key words: The DELTA campaign, the lower thermosphere, temperature and density.

1. Introduction

The dissipation of energy originating in the magnetosphere and lower atmosphere plays an important role in the energy budget controlling the temperature of the polar lower thermosphere (Fujiwara *et al*., 2004). However, correspondence of the time-varying energy dissipation rates to the resulting temperature structure is presently not well investigated. In addition, the vertical structure of temperature is also important for the dynamics in this region. Studies on instability formation and turbulence generation in the neutral wind field require observations of the temperature structure in the background atmosphere. Recent rocket observations in the polar lower thermosphere showed the neutral wind jet with large wind shears during disturbed conditions (Larsen *et al*., 1997), but the mechanisms responsible for generating the jet is still unclear.

In spite of the importance of temperature observation in the lower thermosphere, it is difficult to obtain reliable temperatures from both in situ and remote sensing measurements. The low atmospheric density in this region makes direct measurements difficult, and most techniques infer neutral temperature from Doppler temperature, ion temperature, and rotational temperature on the assumption that the ions, the light-emitting particles, and the rotational state of the molecules, respectively, are in thermal equilibrium with the neutral atmosphere. The Fabry-Perot Interferometer (FPI) derives the neutral temperature from the Doppler width of airglow and auroral emissions, such as green (OI 557.7 nm) and red (OI 630.0 nm) lines. In polar regions, the effective emission altitude of the auroral green line varies depending on the precipitating electron energy. Since vertical temperature gradients in the lower thermosphere are generally steep, there are difficulties in quantitative analysis of the neutral temperature derived from the auroral green line measurement by the FPI. However, the green line temperature measurement is potentially useful in estimating an auroral energy deposition (Holmes *et al*., 2005).

One of the objectives of the Dynamics and Energetics of the Lower Thermosphere in Aurora (DELTA) campaign was to measure temperatures by a rocket-borne instrument, ground-based FPIs, and the European Incoherent Scatter (EISCAT) radar during the auroral disturbances. This paper reports the in situ observations of the rotational temperature and number density of atmospheric molecular nitrogen (N_2) by the N_2 temperature instrument (NTV) onboard the sounding rocket. The N_2 rotational temperature is expected to be equal to the neutral temperature in the lower thermosphere, as described in Section 2.1; thus this experiment provides the vertical structure of the neutral temperature. The results were used to verify quantitatively the FPI tem-

perature measurements.

2. Experiment

2.1 Instrumentation

In situ temperature and density measurements were made with the NTV onboard a sounding rocket during the DELTA campaign. Rocket experiments using this instrument have been successfully carried out twice in Japan (Kawashima *et al.*, 1997; Kurihara *et al.*, 2003). This is an active experiment using the Electron Beam Fluorescence (EBF) technique, and the instrument consists of an electron gun to excite and ionize the ambient N_2 and a spectrometer to detect the fluorescence of the N_2^+ first negative (1N) system. An electron beam with an energy of 1 keV and a current of 10 mA is continuously emitted from the electron gun in a direction perpendicular to the rocket axis, and the excitation-ionization of N_2 and the subsequent fluorescence of the N_2^+ occur along the electron beam. A measurement volume of the NTV is located at an intersection of the electron beam and the field of view of the spectrometer and is 0.2 m away from the payload. The fluorescence spectrum of the N_2^+ 1N system between 380 and 460 nm, including the 1N(0,0) band at 391.4 nm, 1N(1,2) band at 423.7 nm, and 1N(0,1) band at 427.8 nm, is detected by a linear image sensor in the spectrometer. The exposure time for each spectrum is 245.76 ms. The analysis of the fluorescence spectrum provides properties of the initial state of the N_2 molecules: rotational temperature, vibrational temperature, and number density of N_2. The rotational temperature is determined by fitting a synthetic spectrum to the measured spectrum of the 1N(0, 0) band, and the vibrational temperature is determined by measuring the relative intensities of the 1N(0, 1) and 1N(1, 2) bands. The number density is calculated from the intensity of the 1N(0, 0) band. The detailed description of the instrument and measurement method is presented by Kurihara and Oyama (2005).

An equilibrium between rotational and translational degrees of freedom for N_2 is immediately established in the lower thermosphere. Relaxation time for attaining the equilibrium, τ_{RT}, is given by

$$\tau_{RT} = Z_{RT}\, \tau_0, \tag{1}$$

where Z_{RT} is the number of collisions needed for the rotational relaxation and τ_0 is the mean free time between collisions. Values of Z_{RT} for N_2–N_2 collisions in the temperature range of 200–1000 K obtained in the laboratory experiments are 4–14 (Capitelli *et al.*, 2000). The rotational relaxation time τ_{RT} for the N_2 gas is calculated to be $\sim 10^{-3}$ s at 95 km altitude and $\sim 10^{-1}$ s at 140 km. Thus, the rotational temperature of N_2 is expected to be equal to the neutral temperature in the lower thermosphere.

2.2 Rocket experiment

The NTV was installed on the top of the S-310-35 sounding rocket, which was launched northward from Andøya (69.3°N, 16.0°E) at 0:33 UT on 13 December 2004. The temperature and density measurements by the NTV were conducted in at altitude 97–140 km in the ascent of the rocket flight, and after stopping the electron beam emission for 10 s to get the background spectra, the measurements were restarted at altitude 140–95 km in the descent. After that, the temperature and density could not be obtained because the fluorescence spectra were saturated due to the higher atmospheric density. The rocket was separated into mother/daughter payloads at 106.6 km altitude during the ascent. The purpose of the separation is to electrically isolate the other plasma instruments, such as the fast Langmuir probe (FLP) and an impedance probe (NEI), on the mother payload from the NTV on the daughter payload, because the electron beam emission by the NTV causes significant charging of the rocket body.

The experimental conditions for the NTV in the DELTA campaign were different from those in the previous experiments at midlatitudes because of auroral emissions. During the rocket flight, the passages of several auroral arcs were observed by the all-sky camera (ASC) at Kilpisjärvi in the MIRACLE network as shown in Fig. 1. The ASC acquired the images at 557.7 nm with a sampling rate of 20 s. Under such auroral conditions, the background auroral emission can contaminate the spectra observed by the NTV, because the N_2^+ 1N system induced by the EBF technique is commonly seen in auroral spectra. Figure 2(a) and (b) show the spectra observed by the NTV spectrometer during the ascent at 99.7 km and 84.9 km altitude, respectively. Note that the electron beam emission started at 97.3 km during the ascent. The spectra obtained below 97.3 km are not the fluorescence induced by the EBF technique but the background emissions. In Fig. 2(a), the N_2^+ 1N(0, 0), (0, 1), and (1, 2) bands are predominantly strong, and other spectral features are not recognized. Figure 2(b) shows an example of the background auroral emissions, and identifiable bands in Fig. 2(b) are the same as in Fig. 2(a). It is therefore difficult to eliminate the auroral contamination from the observed spectra. The observed intensity of the background auroral emissions changes with altitude and also with look direction of the spectrometer because of the transient and localized nature of the auroral arc, as observed simultaneously by an auroral green line photometer (AGL) onboard the rocket (Iwagami *et al.*, 2006 in this issue). At around 100 km altitude during the ascent, the intensity of the background auroral emission was at least an order of magnitude lower than the intensity of the fluorescence by the EBF technique. However, since the intensity by the EBF technique decreases rapidly with altitude in proportion to the N_2 number density, the auroral emissions can be a significant source of error in the temperature and density measurements at the upper part of the observation, as discussed later.

3. Observational Results

3.1 Rotational temperature and number density of molecular nitrogen

Altitude profiles of the observed N_2 rotational temperature during the ascent and descent of the rocket flight are shown in Fig. 3. The uncertainty in the rotational temperature determination from each spectrum increases with altitude because the signal to noise ratio of the spectrum decreases with a decrease in density. In order to reduce the uncertainty, the spectra are grouped into altitude bins so that the integrated spectra have comparable intensities. As a result, the altitude resolution of the rotational temper-

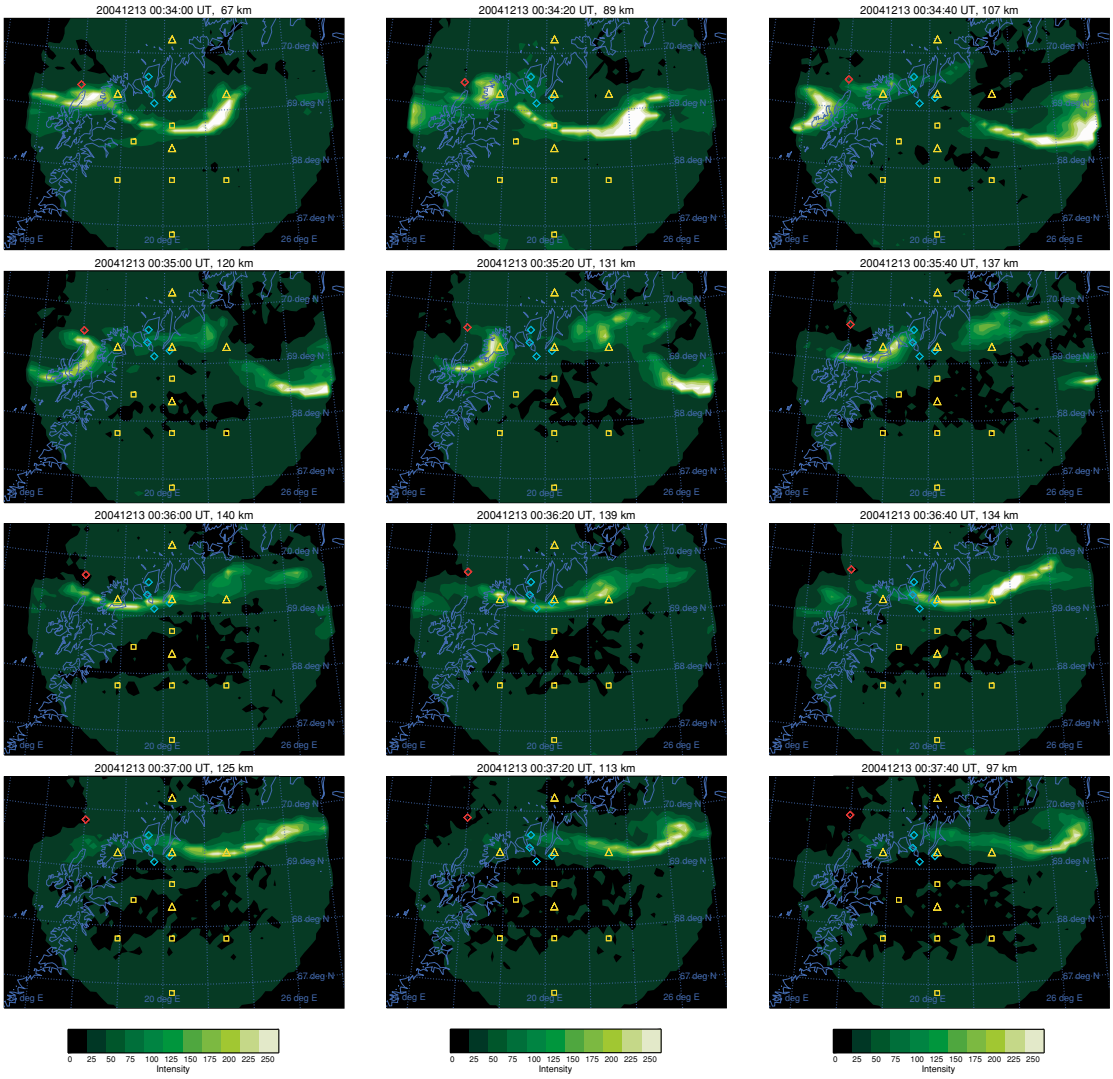

Fig. 1. The green line emissions observed by the ASC at Kilpisjärvi at intervals of 20 s during the rocket flight. The UT time and the corresponding rocket altitude are indicated at the top of each image. The projection altitude of the ASC images, the rocket positions (red diamonds), the EISCAT CP-2 beam positions (cyan diamonds), and the sampled volumes for the Skibotn FPI (yellow triangles) and KEOPS FPI (yellow boxes) is 110 km.

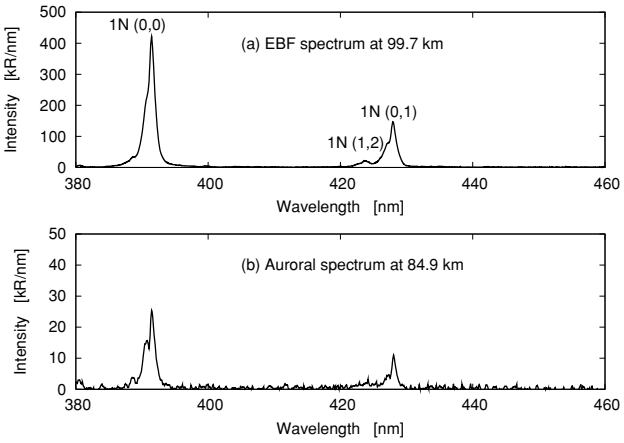

Fig. 2. Spectra from the NTV spectrometer observed at (a) 99.7 km and (b) 84.9 km altitudes. The N_2^+ 1N bands in (a) are the fluorescence mainly induced by the EBF technique, and the same bands in (b) are the background auroral emissions.

ature data in Fig. 3 varies from 1 km at 95 km altitude to 6 km at 140 km. The uncertainty in Fig. 3 is estimated from the signal to noise ratio of the spectrum using the results of the laboratory experiments and increases with altitude from 15 K at 95 km to 40 K at 140 km.

The profiles in the ascent and descent in Fig. 3 agree well above 102 km. Below this altitude, the rotational temperature in the descent is significantly higher than that in the ascent. This enhancement is caused by aerodynamic effects resulting from supersonic motion of the rocket. The temperature of the airflow around the sounding rocket is enhanced by compression depending on the attitude of the rocket (Gumbel, 2001). As mentioned previously, the measurement volume of the NTV is located in the vicinity of the payload, and the rotational temperature measurement can be affected by the translational temperature enhancement around the rocket. Kurihara *et al.* (2006) used the Direct Simulation Monte Carlo (DSMC) method to study the flow around the sounding rocket and the aerodynamic effects on the NTV measurement. These researchers showed that the measurement volume is less than 1 m downstream from

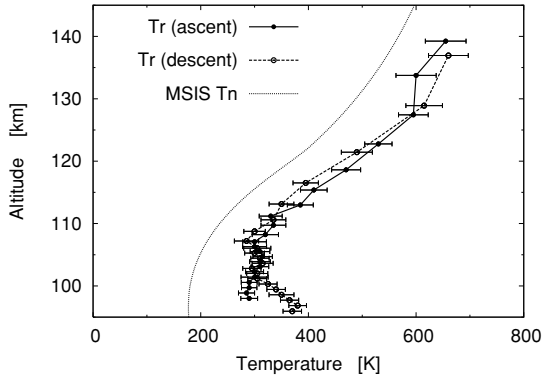

Fig. 3. Observed N_2 rotational temperature profiles during the ascent (solid line) and the descent (dashed line) compared with neutral temperature profile from the MSISE-90 model (dotted line).

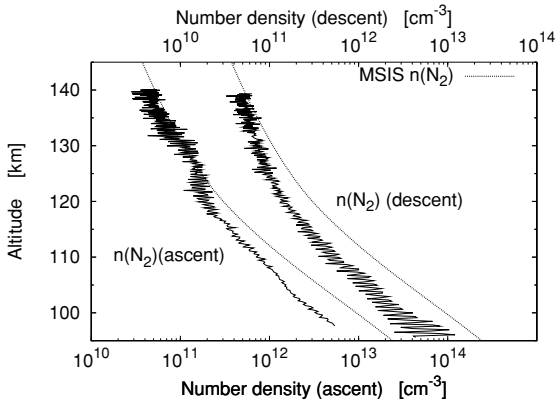

Fig. 4. Observed N_2 number density profiles during the ascent (lower scale) and the descent (upper scale) compared with N_2 number density profile from the MSISE-90 model (dotted lines).

the shock front during the ascent. Atmospheric molecules in the flow travel the distance from the shock front to the measurement volume in $\sim 10^{-3}$ s at the flow speed of ~ 1 km/s. Considering this travel time t and the rotational relaxation time τ_{RT} in Eq. (1), the rotational temperature can be higher than the background neutral temperature below 110 km where $t \simeq \tau_{\mathrm{RT}}$. Above 110 km, the rotational temperature is free from the aerodynamic effects, because the supersonic flow arrives at the measurement volume in a much shorter time than τ_{RT}.

The neutral temperature profile predicted by the Mass Spectrometer Incoherent Scatter (MSISE-90) model (Hedin *et al.*, 1991) is also plotted in Fig. 3. The MSISE-90 model is an empirical model developed to estimate expected values of neutral temperature, number densities of He, O, N_2, O_2, Ar, H, and N, and total mass density as a function of altitude, local time, latitude, longitude, UT, $F_{10.7}$, and A_p. The observed rotational temperature is much higher than the neutral temperature from the MSIS model at all altitudes, and the differences between the rotational temperature and the neutral temperature are 70–140 K above 110 km.

Altitude profiles of the observed N_2 number density are shown in Fig. 4. The ascent and descent data are offset to ease comparison. Unlike the rotational temperature determination, number densities are calculated from each spectrum with a high time resolution of 245.76 ms. Spin periods of the rocket measured by an onboard geomagnetic aspectmeter are ~870 ms during the observation, and hence about four density data are obtained per spin. For this reason, the density profiles in Fig. 4 show clear spin modulation caused by the aerodynamic effect. This spin modulation in the density profiles is a ram/wake modulation, which is caused by the compression/rarefaction typically observed by side-looking instruments (Gumbel, 2001). Similar spin modulation observed in the previous NTV experiment at the midlatitude was quantitatively analyzed by Kurihara *et al.* (2006). The amplitude of the spin modulation during the descent is larger than that during the ascent, particularly in the lower altitudes, because an angle of attack of the rocket is larger during the descent.

As in the case of the rotational temperature profiles, the density profiles during the ascent and descent indicate a similar tendency. However, at altitude 120–135 km the density during the ascent is higher than that during the descent. This is mainly attributed to the auroral contamination of the observed spectra. The projections of the auroral arcs observed by the Kilpisjärvi all-sky camera in Fig. 1 show that the auroral arc was located just on the south side of the rocket during the ascent and moved eastward during the descent. The AGL onboard the rocket also detected larger slant emission rates of the green line during the ascent (Iwagami *et al.*, 2006 in this issue).

In order to estimate the auroral contamination in the NTV spectra, the difference of the density profiles between the ascent and descent is converted to the original 1N(0, 0) band intensity and compared with the slant emission rate of the auroral green line observed by the AGL in Fig. 5. Although the AGL was installed on the daughter payload, the AGL and NTV look in approximately the same direction away from the rocket axis. The angles between the rocket axis and the line of sight of the AGL and NTV are 60.0 and 67.5 degrees, respectively. The 1N(0,0) band intensity and the slant emission rate of the green line in Fig. 5 are shown as differences in the spin-averaged profiles between the ascent and descent. The 1N(0, 0) band profile is similar to the green line above 105 km. This result implies that most of the density difference between the ascent and descent is due to the auroral contamination and that the true density profiles during the ascent and descent are very similar. The dissimilarity between the 1N(0,0) band and the green line emission profiles below 105 km in Fig. 5 results from the large spin modulation on the density profile during the descent. Kurihara *et al.* (2006) performed the numerical simulation of the spin modulation on the density measured by the NTV in the previous experiment and showed that the simple running average of the spin modulation deviates from the true background atmospheric density when the amplitude of the spin modulation is large.

The observed density profiles are also compared with the density profile from the MSIS model. The observed N_2 number density profiles both during the ascent and descent are lower than the N_2 number density values from the MSISE-90 model at all altitudes as shown in Fig. 4. The observed density during the descent, which is much less affected by the auroral contamination, gradually approaches

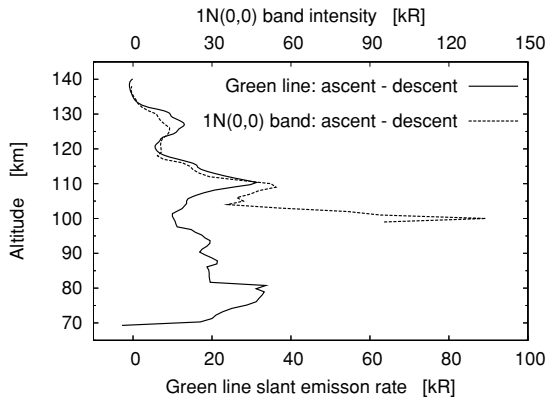

Fig. 5. Slant emission rate of the green line observed by the AGL (solid line) and the 1N(0,0) band intensity observed by the NTV (dashed line). Both are differences of the spin-averaged profiles between the ascent and descent.

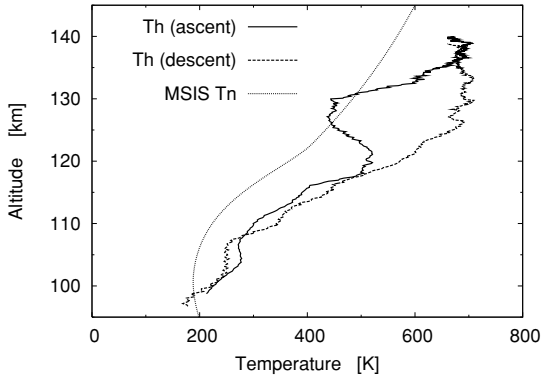

Fig. 6. Neutral temperature profiles during the ascent (solid line) and the descent (dashed line) derived from the observed N_2 number densities and the assumption of hydrostatic equilibrium. The MSISE-90 model temperature profile (dotted line) is also shown for comparison.

the MSISE-90 density with altitude from $\sim$ 30% at 95 km to $\sim$ 90% at 140 km.

If the atmosphere is in hydrostatic equilibrium, lower densities are generally consistent with higher temperatures because higher temperatures lead to larger scale heights. From the hydrostatic equation combined with the ideal gas law, the neutral temperature profile $T(z)$ can be deduced by integrating the total number density profile $n(z)$,

$$T(z) = \frac{1}{n(z)} \left\{ n(z_0)\, T(z_0) - \frac{1}{k} \int_{z_0}^{z} g(z)\, n(z)\, m(z)\, dz \right\}, \qquad (2)$$

where k is the Boltzmann constant, $g(z)$ is the acceleration of gravity, and $m(z)$ is the mean molecular mass. The integration in Eq. (2) is performed from the upper boundary of the altitude range, z_0, to the altitude of interest, z. This method is applied to the present observation. The total number density profile is derived from the spin-averaged profile of the observed N_2 number density using the ratio of total and N_2 number densities calculated from the MSISE-90 model. The values of $m(z)$ are also obtained from the MSIS model. The value of the neutral temperature at the upper boundary is taken to be equal to the rotational temperature at the top of the observation.

Possible sources of error in this method are the auroral contamination and the aerodynamic effects on the observed N_2 number density and the deviation from the MSIS model composition. The quantitative estimation of aerodynamic effects on the N_2 number density measurements requires a three-dimensional numerical simulation of the flow around a sounding rocket. The simulation by Kurihara *et al.* (2006) showed that the absolute number densities are about 10% lower than the spin-averaged number density below an altitude of 130 km during the ascent. However, the temperature derivation in Eq. (2) is little affected by such a systematic error in the density because a constant percentage error is canceled, as is obvious from Eq. (2). The composition model is of minor importance below an altitude of 120 km where the mean molecular mass is nearly constant.

Figure 6 shows the neutral temperature profiles derived from the observed N_2 number densities and the assumption of hydrostatic equilibrium. The neutral temperatures in the ascent and descent agree well below 120 km, but they differ considerably at 120–135 km. The major cause of this difference is the auroral contamination present in the N_2 number density measurements. Below 120 km, the auroral intensities are relatively small compared with the fluorescence induced by the NTV. The derived neutral temperatures are consistent with the observed rotational temperatures in Fig. 3 in the 110–120 km region where both results are reliable. Below 110 km, the difference between the neutral and rotational temperatures grows larger as the altitude decreases. This result demonstrates that the rotational temperature is actually enhanced by the aerodynamic effects with a decrease in the rotational relaxation time τ_{RT} in Eq. (1) and that the rotational temperature measurement is free from the aerodynamic effects above 110 km, as expected theoretically.

3.2 Neutral temperature

The two ground-based FPIs at Skibotn (69.3°N, 20.4°E) and the Kiruna Esrange Optical Platform System (KEOPS) site (67.8°N, 20.4°E) sampled the auroral green line emission at 557.7 nm and provided neutral temperatures and line of site wind velocities. Both FPIs operated a normal scan of cardinal directions plus zenith, but the KEOPS FPI had one extra direction of Northwest towards the rocket trajectory, as shown in Fig. 1. A detailed description of the instruments and observations is presented by Griffin *et al.* (2006) in this issue. The neutral temperatures measured from the two directions closest to the sounding rocket, the Skibotn West and the KEOPS Northwest, at the period from 23:00 UT on 12 to 2:00 UT on 13 December 2004 are shown in figure 11 of Griffin *et al.* (2006). The temperatures from two directions are in very good agreement at $\sim$500 K just before the launch time. The Skibotn West data show a temperature jump of 150 K at 0:36:37 UT just after the launch and return to the former 500 K level at the next data point in 7.5 min. The KEOPS Northwest temperature gradually increases after the launch time up to $\sim$600 K and drops to $\sim$300 K after 1:15 UT. The data from the other directions show a temperature of around 500 K during the rocket flight.

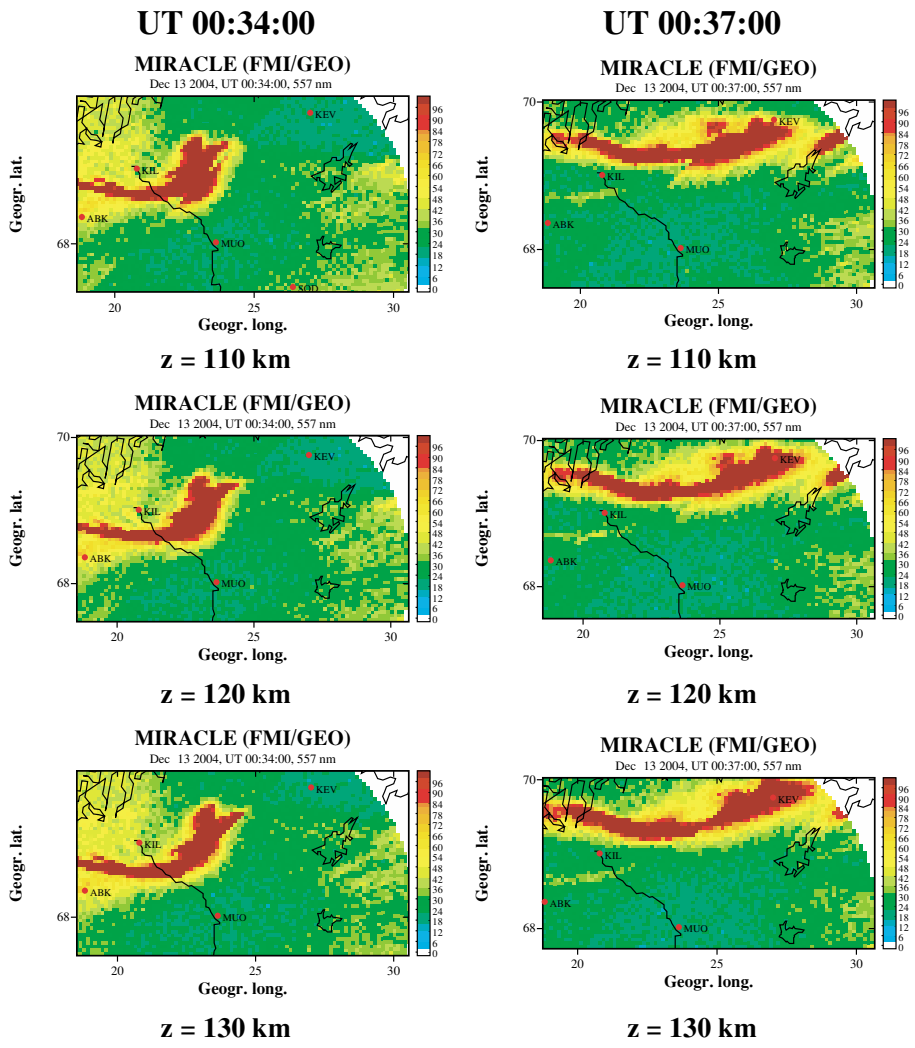

Fig. 7. Combined ASC images for the projection altitude of 110, 120, and 130 km at 0:34 and 0:37 UT on 13 December 2004. The two ASC images from Kilpisjärvi (KIL) and Muonio (MUO) are combined on the middle line between the two stations. The combined images for 120 km show smooth connections of the continuous arc than those for 110 and 130 km.

3.3 Auroral emission height

The two ASCs at Kilpisjärvi (69.0°N, 20.9°E) and Muonio (68.0°N, 23.5°E) in the MIRACLE network acquired the green line emissions simultaneously. The combination of the two ASC images can be used to determine the altitude of auroral arcs by a stereo imaging technique. Figure 7 shows the combined ASC images for different projection altitudes at 0:34 and 0:37 UT on 13 December 2004. The two ASC images from Kilpisjärvi and Muonio are combined on the middle line between the two stations. The combined images for the projection altitude of 120 km show better connections of the continuous arc at the seam of the two ASC images than those for 110 and 130 km. These results suggest that the effective altitude of the auroral arc at around the time of the launch is about 120 km.

4. Discussion

The results of the observations of the rotational temperature and number density of N_2 in the DELTA campaign have features different from the MSIS model values. The observed rotational temperature is 70–140 K higher than the neutral temperature from the MSIS model above 110 km in the DELTA campaign. On the other hand, the observed N_2 number density is significantly lower than the MSIS model value, especially in lower altitudes. Although the rotational temperature measurement below 110 km is affected by aerodynamic effects, the independent neutral temperature profile is derived by integrating the N_2 density profile based on the assumption of the hydrostatic equilibrium. The derived neutral temperatures in the ascent are 220 K at 100 km and 275 K at 105 km. These values are lower than the observed rotational temperatures but higher than the mean temperatures in December observed by the sodium lidar at Andøya and reported by Lübken and von Zahn (1991), which yielded 190 K at 100 km and 193 K at 105 km and was close to the MSIS model. Even considering uncertainties due to the measurement methods, the temperature observed by the present rocket experiment is evidently enhanced by some geophysical processes not only above 110 km but also in the range of 100–110 km. The temperature enhancement can be influenced by Joule heating and particle precipitation events around the launch time of the rocket. The EISCAT radar observation suggested that an intense Joule heating due to the presence of the strong elec-

tric field and the high electron density in the E region started 30 min before the launch (Nozawa *et al.*, 2006 in this issue). Even though the cause of the observed N_2 density reduction is unclear, lower densities contribute to larger temperature enhancements for a certain rate of the energy input per unit volume. The particle heating makes more local and temporary contributions to the temperature enhancements, as seen in the ASC images of auroral arcs in Fig. 1. The MSIS model is an empirical atmospheric model based on existing observational data and, in many cases, shows good agreement with statistical observations, but it cannot accurately reproduce temporal atmospheric disturbances within a few hours. In the present observation, intense Joule and particle heating events around the launch time are possible candidates of large temperature and density deviations from the MSIS model and Lübken and von Zahn (1991).

The temperature values from the MSIS model in the lower thermosphere is based on the assumption that the neutral temperature is equal to the ion temperature. The validity of this assumption during the geomagnetically disturbed period can be checked by comparing the rotational temperature with the ion temperature observed by the EISCAT radar during the DELTA campaign. A detailed comparison is provided in Nozawa *et al.* (2006) in this issue. The EISCAT ion temperature is 200 K higher at and above 120 km than the neutral temperature from the NTV, but the altitude profiles are similar. Since the strength of the electric field was about 50 mV/m and the agreement is good below 110 km, these authors suggested that the ion/rotational temperature difference above 110 km is caused by Joule heating. They also derived neutral temperatures from the EISCAT ion temperature using the steady state ion energy equation and found good agreement for neutral temperatures measured by the NTV and derived by the EISCAT radar observations at and below 110 km. The ion temperature retrieved from incoherent scatter spectra is influenced by the ion-neutral collision frequency. The ion-neutral collision frequency depends on the neutral density and composition, so that the large deviation of the observed N_2 number density from the MSIS model value can affect the estimation of the ion temperature. Maeda *et al.* (2005) discussed the effect of the assumed ion-neutral collision frequency on the ion temperature derived from the EISCAT-UHF radar at Tromsø and the ESR at Longyearbyen. They showed that the underestimate (overestimate) of the ion-neutral collision frequency resulted in the overestimate (underestimate) of the ion temperature around 100 km altitude; this was particularly true for the periods of strong electric fields. In addition, the change in the ion-neutral collision frequency can produce significant effects on the estimation of the E region neutral wind, conductivities, ionospheric current, and thereby the electromagnetic energy transfer rate, from the EISCAT measurements (Fujii *et al.*, 1998).

Large deviations from the MSIS model were also observed in previous experiments at the midlatitude (Kawashima *et al.*, 1997; Kurihara *et al.*, 2003). The largest differences reached a 150 K increase in temperature and a 50% decrease in density at an altitude of 115 km. These deviations are comparable to those in the DELTA campaign. In contrast, above altitude 130 km in the midlatitude observations, the temperature and density were lower and higher, respectively, than the MSIS model. The results of the NTV experiments in the midlatitude and polar region show that the observed large deviations in the temperature and density from the MSIS model are less likely to be systematic errors inherent in the NTV experiment or the MSIS model and are common in the lower thermosphere.

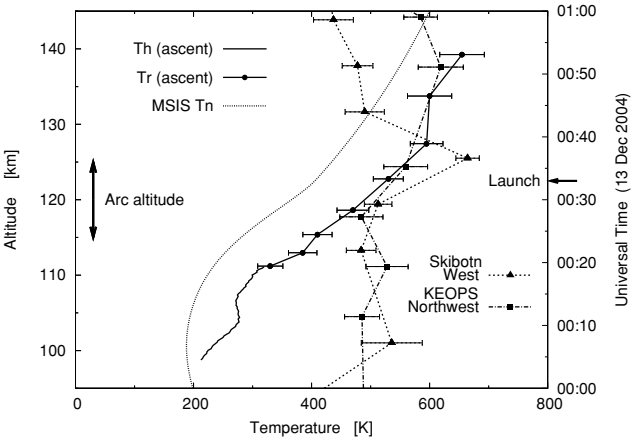

Fig. 8. Comparison of the in situ and FPI temperature observations. The rotational temperature and neutral temperature from the NTV (solid line) and the neutral temperature from MSISE-90 model (dotted line) are plotted as a function of altitude (left scale), and the neutral temperatures from the Skibotn West (dashed line) and the KEOPS Northwest (dot-dashed line) directions are plotted as a function of universal time on 13 December 2004 (right scale). The effective altitude of the auroral arc determined from the combined ASC images and the time of the rocket launch are also represented by the arrows.

The auroral contamination in the observed spectra cannot be easily eliminated, but it becomes evident from the comparison with the green line emission measurement by the AGL that the density difference between the ascent and descent is mostly caused by the auroral contamination. In other words, the density profiles during the ascent and descent turned out to be very similar. It is not easy to estimate the effect of the auroral contamination on the rotational temperature measurement, but the actual differences in the observed rotational temperature between the ascent and descent are within the margin of uncertainty. Judging from the results of the in situ observations, the neutral atmosphere was fairly uniform, at least along the rocket trajectory.

The temperatures from the in situ observation and from the ground-based FPI observation are compared in Fig. 8. For the in situ observation, the rotational temperature observed above 110 km during the ascent is presented as is the neutral temperature derived from the observed N_2 number density and the assumption of hydrostatic equilibrium below 110 km during the ascent. The effective altitude of the auroral arcs during the rocket flight is determined to be $\sim$120 km from the combinations of the two ASC images at Kilpisjärvi and Muonio in Fig. 7, and this altitude corresponds to the rotational temperature of $\sim$500 K at 120 km, as shown in Fig. 8. The FPI neutral temperatures in Fig. 8 are limited to the observation of the two directions closest to the sounding rocket, the Skibotn West and the KEOPS Northwest, at the period from 0:00 UT on 12 to 1:00 UT

on 13 December 2004. As described previously, the FPI neutral temperatures are at 500 K level except for the time just after the launch. The reason for this deviation is investigated in detail by Griffin *et al*. (2006) in this issue. Even if the observed temperature jump to ∼650 K for the Skibotn West is an actual neutral temperature enhancement at 120 km, the temperature jump is a local enhancement owing to some localized heating mechanisms such as a particle heating because the KEOPS Northwest temperature is at the 550 K level around that time. As a result, the neutral temperature from the ground-based FPI observations is consistent with the observed rotational temperature rather than with the MSIS model profile. This conclusion is consistent with the EISCAT-FPI results of Kosch *et al*. (2000).

It should be noted that the temperature jump for the Skibotn West in the FPI observation is a reliable result with a small error bar. Griffin *et al*. (2006) discussed the temperature peaks between 23:00 on 12 and 2:00 UT on 13 December. It is difficult, however, to simply conclude that the temperature peaks are caused by either changes in the auroral emission height or some localized heating mechanisms, because the rocket trajectory and the sampled volumes of the FPIs do not ovelap directly. Further studies including high spatial and time resolution simulations of a moving auroral arc are necessary to explain these observations.

5. Summary

The rotational temperature and number density of N_2 in the polar lower thermosphere were observed with the rocket-borne NTV in the DELTA campaign. The observed rotational temperature is 70–140 K higher than the MSIS model above 110 km, where the aerodynamical effects on the rotational temperature measurement are negligible. The observed N_2 number density during the descent, when the auroral contamination was sufficiently small, is much lower than the MSIS model and changes with altitude from 30% at 95 km to 90% at 140 km. This density reduction from the MSIS model density has a significant impact on the use of the ion-neutral collision frequency in EISCAT observations and thereby on the estimation of the ion temperature, neutral wind, ionospheric current, and electromagnetic energy transfer rate. The results of the NTV observation in the DELTA campaign and the previous midlatitude experiments show that large temperature and density deviations from the MSIS model are commonly seen in the lower thermosphere. The similarity of the profiles between the ascent and descent for both the rotational temperature and number density indicate that the neutral atmosphere was horizontally uniform along the rocket trajectory.

The results of the in situ observations are compared with the FPI temperature observation. The effective altitude of the auroral arcs during the flight are determined to be ∼120 km from the combined ASC images, because the combined images for the projection altitude of 120 km show better connections of the continuous arc at the seam of the two ASC images than those for 110 and 130 km. The neutral temperature of ∼500 K from the ground-based FPI observations just before the launch time is consistent with the observed rotational temperature at 120 km rather than the MSIS model profile. Further studies are needed to clarify the cause of the temperature peaks in the FPI observations after the launch time, because the rocket trajectory and the sampled volumes of the FPIs do not overlap directly.

Acknowledgments. The authors thank the rocket launching group of ISAS and all related government institutions for conducting the successful experiments. This work was carried out by the joint research program of the Solar-Terrestrial Environment Laboratory, Nagoya University.

References

Capitelli, M., C. M. Ferreira, B. F. Gordiets, and A. I. Osipov, *Plasma Kinetics in Atmospheric Gases*, Springer series on atomic, optical, and plasma physics, 31, Springer, New York, 300 pp, 2000.

Fujii, R., S. Nozawa, N. Matuura, and A. Brekke, Study on neutral wind contribution to the electrodynamics in the polar ionosphere using EISCAT CP-1 data, *J. Geophys. Res.*, **103**, 14731–14739, 1998.

Fujiwara, H., S. Maeda, M. Suzuki, S. Nozawa, and H. Fukunishi, Estimates of electromagnetic and turbulent energy dissipation rates under the existence of strong wind shears in the polar lower thermosphere from the European Incoherent Scatter (EISCAT) Svalbard radar observations, *J. Geophys. Res.*, **109**, A07306, doi:10.1029/2003JA010046, 2004.

Griffin, E., M. Kosch, A. Aruliah, A. Kavanagh, I. McWhirter, A. Senior, E. Ford, C. Davis, T. Abe, J. Kurihara, K. Kauristie, and Y. Ogawa, Combined ground-based optical support for the aurora (DELTA) sounding rocket campaign, *Earth Planets Space*, **58**, this issue, 1113–1121, 2006.

Gumbel, J., Aerodynamic influences on atmospheric in situ measurements from sounding rockets, *J. Geophys. Res.*, **106**, 10553–10563, 2001.

Hedin, A. E., Extension of the MSIS thermosphere model into the middle and lower atmosphere, *J. Geophys. Res.*, **96**, 1159–1172, 1991.

Holmes, J. M., M. Conde, C. Deehr, and D. Lummerzheim, Morphology of evening sector aurorae in λ557.7-nm Doppler temperatures, *Geophys. Res. Lett.*, **32**, L02103, doi:10.1029/2004GL021553, 2005.

Iwagami, N., S. Komada, and T. Takahashi, Preliminary results of rocket attitudes and auroral green line emission rates in the DELTA campaign, *Earth Planets Space*, **58**, this issue, 1107–1111, 2006.

Kawashima, T., K.-I. Oyama, K. Suzuki, N. Iwagami, and S. Teii, A measurement of the N_2 number density and the N_2 vibrational rotational temperature in the lower thermosphere—Instrumentation and preliminary results, *Adv. Space Res.*, **19**, 663–666, 1997.

Kosch, M. J., M. Ishii, S. Nozawa, D. Rees, K. Cierpka, A. Kohsiek, K. Schlegel, R. Fujii, T. Hagfors, T. J. Fuller-Rowell, and C. Lathuillere, A comparison of thermospheric winds and temperatures from Fabry-Perot interferometer and EISCAT radar measurements with models, *Adv. Space Res.*, **26**, 979–984, 2000.

Kurihara, J. and K.-I. Oyama, Rocket-borne instrument for measuring vibrational-rotational temperature and density in the lower thermosphere, *Rev. Sci. Instrum.*, **76**, 083101, doi:10.1063/1.1988189, 2005.

Kurihara, J., K.-I. Oyama, K. Suzuki, and N. Iwagami, Vibrational-rotational temperature measurement of N_2 in the lower thermosphere by the rocket experiment, *Adv. Space Res.*, **32**, 725–729, 2003.

Kurihara, J., K.-I. Oyama, N. Iwagami, and T. Takahashi, Numerical simulation of 3D flow around sounding rocket in the lower thermosphere, *Ann. Geophys.*, **24**, 89–95, 2006.

Larsen, M. F., A. B. Christensen, and C. D. Odom, Observations of unstable atmospheric shear layers in the lower E region in the post-midnight auroral oval, *Geophys. Res. Lett.*, **24**, 1915–1918, 1997.

Lübken, F.-J. and U. von Zahn, Thermal structure of the mesopause region at polar latitudes, *J. Geophys. Res.*, **96**, 20841–20857, 1991.

Maeda, S., S. Nozawa, Y. Ogawa, and H. Fujiwara, Comparative study of the high-latitude E region ion and neutral temperatures in the polar cap and the auroral region derived from the EISCAT radar observations, *J. Geophys. Res.*, **110**, A08301, doi:10.1029/2004JA010893, 2005.

Nozawa, S., Y. Ogawa, A. Brekke, T. Tsuda, C. M. Hall, H. Miyaoka, J. Kurihara, T. Abe, and R. Fujii, EISCAT observational results during the DELTA campaign, *Earth Planets Space*, **58**, this issue, 1183–1191, 2006.

J. Kurihara (e-mail: kuri@isas.jaxa.jp), T. Abe, K. Oyama, E. Griffin, M. Kosch, A. Aruliah, K. Kauristie, Y. Ogawa, S. Komada, and N. Iwagami